

Coherent and Incoherent States of Electron-doped SrTiO₃

Yukiaki Ishida,¹ Ritsuko Eguchi,¹ Masaharu Matsunami,¹ Koji Horiba,¹ Munetaka Taguchi,¹ Ashish Chainani,¹ Yasunori Senba,² Haruhiko Ohashi,² Hiromichi Ohta,³ and Shik Shin^{1,4}

¹RIKEN SPring-8 Center, Sayo, Sayo, Hyogo 679-5148, Japan

²JASRI/SPring-8, Sayo, Sayo, Hyogo 679-5198, Japan

³Graduate School of Engineering, Nagoya University, Furo, Chikusa, Nagoya, Aichi 464-8603, Japan

⁴ISSP, University of Tokyo, Kashiwa-no-ha, Kashiwa, Chiba 277-8561, Japan

(Dated: October 27, 2018)

Resonant photoemission at the Ti 2*p* and O 1*s* edges on a Nb-doped SrTiO₃ thin film revealed that the coherent state (CS) at the Fermi level (E_F) had mainly Ti 3*d* character whereas the incoherent in-gap state (IGS) positioned ~ 1.5 eV below E_F had mixed character of Ti 3*d* and O 2*p* states. This indicates that the IGS is formed by a spectral-weight transfer from the CS and subsequent spectral-weight redistribution through *d-p* hybridization. We discuss the evolution of the excitation spectrum with 3*d* band filling and rationalize the IGS through a mechanism similar to that proposed by Haldane and Anderson.

PACS numbers:

SrTiO₃ (STO) is a perovskite-type oxide semiconductor with a band gap of 3.2 eV [1] and is considered to be one of the promising device materials in “oxide electronics.” A variety of transition-metal oxides can be grown on STO with atomical flatness to show novel phenomena such as the high-mobility and magnetic interface of LaAlO₃/STO [2, 3] and state-of-the-art thermoelectric performance of STO:Nb/STO superlattice [4]. Additionally, carrier (electron) concentration of STO is controllable through substitutional doping or through a field effect [5], as performed in conventional semiconductor-device materials.

While band theory may be a starting point to understand the transport and magnetic properties of lightly-doped STOs [6], their electronic structures near the Fermi level (E_F) are far from being doped band insulators: photoemission spectroscopy (PES) studies [7, 8, 9, 10, 11] have revealed incoherent states forming in the band gap of STO (in-gap states: IGSs) instead of a rigid shift of the bands with increasing the conduction-band filling x as schematically shown in Fig. 1(a). Since the system shows a metal-insulator transition with $x \rightarrow 1$ and the end member is a correlated d^1 insulator such as LaTiO₃ [6] (a Mott-Hubbard-type insulator in the Zaanen-Sawatzky-Allen scheme [12]), the IGSs in the metallic phase may be viewed as precursors of the “lower-Hubbard band” of the d^1 insulators [13]. However, a Hubbard model, which produces incoherent states through electron correlation as shown in Fig. 1(b), is insufficient to explain the IGSs [7, 14, 15] since they are observed already at $x \sim 0.05$ [10] where electron correlation is expected to be small [6]. The origin of the IGSs at $x \sim 0$ was attributed to chemical disorder [11], polaron effect [16], or partly to donor levels [9], but no consensus has been reached yet (see p. 1171 of [17]).

In this Letter, we investigate the origin of the IGSs of lightly-electron-doped STO using soft-x-ray resonant PES, which is a convenient tool to obtain the partial density of states (PDOS) in the valence-band spectra [18].

By performing resonant PES at the Ti 2*p* and O 1*s* edges, we find not only Ti 3*d* character but also O 2*p* character in the IGSs, which is direct evidence for *d-p* hybridization playing an important role for the existence of the IGSs, whereas the coherent states at E_F has mainly Ti 3*d* character. In contrast to the picture that the IGSs and the coherent states are resulting from correlations within the conduction electrons as schematically shown in Fig. 1(b), we assign them to locally-screened and non-locally-screened final states, respectively, as shown in Fig. 1(c). The IGSs are considered qualitatively equivalent to the multiple charge states of transition-metal impurities in semiconductors accumulating in the middle of the band gap with increasing hybridization as proposed by Haldane and Anderson [19].

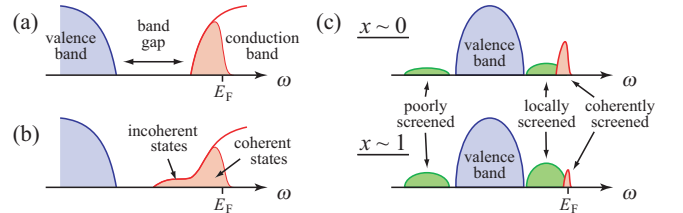


FIG. 1: Schematic electronic structures near E_F within band theory (a), when correlation effects are included for the conduction electrons (b), and within a model including various screening channels (c).

A 100-nm thick STO:Nb film was grown epitaxially on a (100) face of insulating LaAlO₃ by a pulsed laser deposition method [20]. The carrier concentration was estimated to be $\sim 1 \times 10^{21}$ cm⁻³ or $x \sim 0.06$ (see below). Soft-x-ray absorption (XAS) and PES measurements were performed at 50 K at undulator beamline BL17SU of SPring-8 equipped with a Gammadata-Scienta SES2002 analyzer [21]. The incident light was circularly polarized. The PES spectra were recorded at ~ 250 -meV energy resolution and the binding energies (E_B 's) were referenced

to E_F of gold in contact with the sample and the analyzer. An STO film grown on an STO:Nb/LaAlO₃ was also measured. The sample surface was reasonably clean without any surface treatment, as described below.

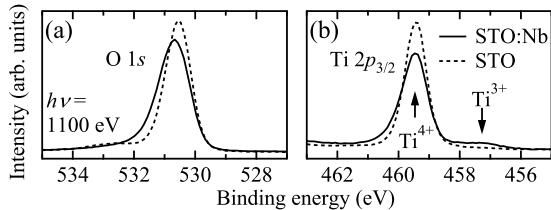


FIG. 2: O $1s$ (a) and Ti $2p_{3/2}$ (b) core-level spectra.

Figure 2 shows core-level spectra of STO:Nb and STO. The O $1s$ spectrum of STO:Nb was a single peak at $E_B = 530.7$ eV ($\equiv E_{1s}$) with an asymmetry due to metallic screening. A hump feature at $E_B \sim 533$ eV was negligible, indicating that the sample surface was fairly clean. The Ti $2p_{3/2}$ spectrum of STO:Nb showed a weak Ti³⁺ peak at ~ 2 eV below the main Ti⁴⁺ peak at $E_B = 459.5$ eV. From the intensity ratio of Ti³⁺/Ti⁴⁺ peaks [14, 15], we deduced $x = 0.06 \pm 0.02$. This value was consistent with $x < 0.1$ estimated from the Ti $2p$ XAS line-shape broadening [Fig. 3(a)], which is a measure of the content of Ti³⁺ component [22]. Since STO:Nb is a paramagnetic metal, we interpret that the valence of Ti is fluctuating between 3+ and 4+ with a time scale longer than that characteristic of a photoemission process ($\sim 10^{-16}$ s) [23], and PES provides a snapshot of this fluctuation to give a double-peaked Ti $2p$ spectrum. Alternatively, the photoemission initial state of STO:Nb is well described as a fraction x of the Ti sites have nominally- d^1 configuration and the rest have nominally- d^0 configuration. Later, we will use this picture in explaining the excitations near E_F .

Valence-band spectra recorded around the Ti $2p_{3/2}$ absorption edge are shown in Fig. 3(b). At $h\nu = 458.1$ eV, resonant enhancement was observed in the O $2p$ band region [the ~ 6 -eV-wide structure centered at $E_B = 6.5$ eV ($\equiv E_{2p}$)] and in the near- E_F region ($E_B < 3$ eV.) In the O $2p$ band region, the higher- E_B side showed stronger enhancement reflecting Ti $3d$ -O $2p$ bonding character as described by band theory [24, 25, 26]. The enhanced structures at $h\nu = 458.1$ eV in the near- E_F region consisted of a peak at E_F and a broad structure centered at ~ 1.5 eV, which are the coherent states and the IGs of doped STO, respectively [7, 8, 9, 10, 11]. We also confirmed that the resonantly enhanced IGs were dominated by bulk character states from the take-off-angle (θ) dependence of the spectra at $h\nu = 458.1$ eV as shown in Fig. 3(c). Note that, if the ~ 1.5 -eV state was due to surface states, the intensity should scale, with decreasing bulk sensitivity (with increasing θ), to that of the 11-eV peak which originates from surface adsorbates [27]. This is clearly not the case as seen in Fig. 3(c), where

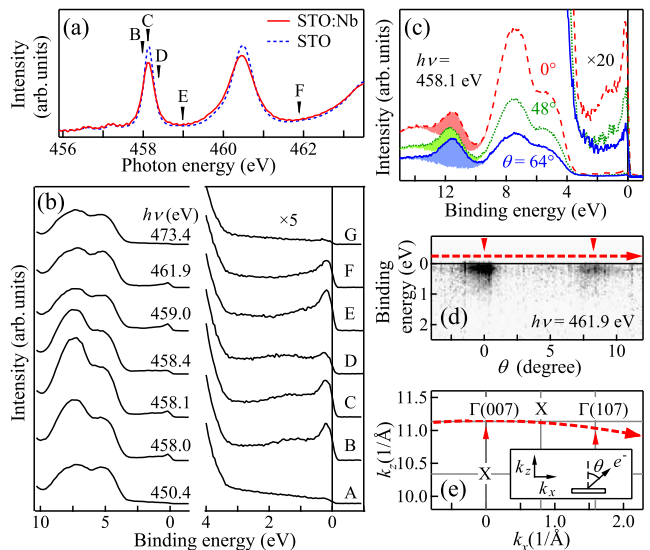


FIG. 3: Resonant PES at the Ti $2p_{3/2}$ absorption edge. (a) Ti $2p_{3/2}$ XAS of STO:Nb and STO. (b) Valence-band spectra of STO:Nb at the Ti $2p_{3/2}$ absorption edge. The intensities were normalized to the photon flux (post-focusing mirror current). The labels on the spectra (B to F) correspond to photon energies indicated in (a). (c) Take-off-angle dependence of the valence-band spectra taken in the angle-integrated mode at $h\nu = 458.1$ eV. Spectra were normalized to the ~ 11 -eV peak area (colored area.) (d) Dispersion recorded in the angle-resolved mode along a trace in the momentum space shown by a dotted line in panel (e). Black/white corresponds to high/low intensity. Triangles indicate electron pockets detected around the Γ points. Inset in (e) defines θ and coordinate of the momentum vector.

the intensity at $E_B < \sim 2$ eV scales with the O $2p$ band intensity.

In Fig. 3(b), one can also see enhancement of the coherent state in the spectra recorded at $h\nu = 459.0$ and 461.9 eV. This is attributed to normal-emission angle-resolved effect, that is, an electron pocket around the Γ point was crossed at $h\nu \sim 460$ eV. In fact, we confirmed the electron pockets around the Γ points in an off-normal angle-resolved PES measurement at $h\nu = 461.9$ eV, as shown in Fig. 3(d). Using an inner potential 12 ± 1 eV measured from E_F [10], the c -axis lattice parameter was 3.94 ± 0.02 Å, which is in good agreement with that derived from x-ray diffraction measurements [20]. The dispersion observed in the angle-resolved PES spectra is a sign of good crystallinity of the sample surface.

Figure 4(a) shows O $1s$ XAS of STO:Nb and STO. The O $1s$ XAS line shape of STO is in good agreement with that reported by de Groot *et al* [28]. The overall line shape except for the sharpness of the peak at $h\nu \sim 533.2$ eV as indicated by a square in Fig. 4(a) was well reproduced by the oxygen- p -projected unoccupied density of states of STO calculated using a local-density approximation [28]. The sharp peak at $h\nu \sim 533.2$ eV

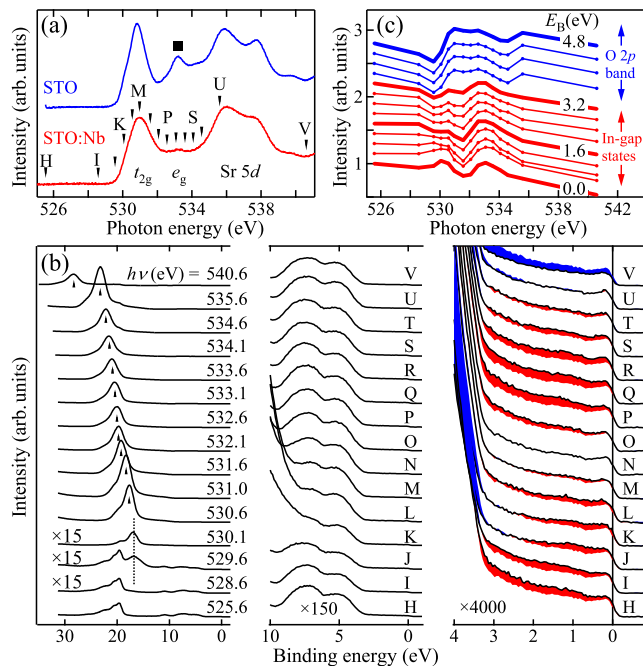


FIG. 4: Resonant PES at the O $1s$ absorption edge. (a) O $1s$ XAS of STO:Nb and STO. The structures at $h\nu = 530.9$, 533.2, and 534.5–538.5 eV corresponds to O $1s$ core-electron excitation into O $2p$ states hybridized with Ti $3d t_{2g}$, Ti $3d e_g$, and Sr $5d$ states, respectively. (b) Valence-band spectra at the O $1s$ absorption edge. The labels on the spectra (H to V) correspond to the photon energies indicated in (a). The triangles in the left panel indicate the O $KL_{2,3}L_{2,3}$ Auger peak positions. The red (light grey) and blue (dark grey) area in the right panel indicate positive and negative differences to the 531.6-eV spectrum. The structures around 20 and 22 eV are due to Sr $4p$ and O $2s$ core levels, respectively. (c) CIS spectra. Each spectrum is normalized to the intensity at 525.6 eV and has an arbitrary offset.

appearing in the excitation region of O $1s \rightarrow$ O $2p$ states hybridized into Ti $3d e_g$ states was attributed to the O $1s$ core hole in the XAS final state [28]: the electron excited into the e_g band is strongly influenced by the O $1s$ core-hole potential through large Ti $3d e_g$ -O $2p$ hybridization to form a core-excitonic state. The peak at $h\nu \sim 533.2$ eV is suppressed and broadened in the spectrum of STO:Nb [Fig. 4(a)], indicating that the life time of the core-excitonic state became shorter due to metallic screening. Nevertheless, the peak at $h\nu \sim 533.2$ eV is still observed in the spectrum of STO:Nb, indicating that the localized XAS final state is still present. Indeed, the resonant enhancement in the near- E_F spectra occurs at $h\nu \sim 533.2$ eV as described below.

Figure 4(b) shows valence-band spectra recorded around the O $1s$ absorption edge. For $h\nu \geq 530.1$ eV, intense O $KL_{2,3}L_{2,3}$ Auger emission [29, 30, 31, 32, 33] appeared and the peak position ($\equiv E_{KLL}$) shifted to higher E_B 's with increasing $h\nu$'s. The O $2p$ on-site

Coulomb interaction was estimated to be $U_{pp} \sim 5.5$ eV using the relationship $U_{pp} = E_{1s} - (h\nu - E_{KLL}) - 2E_{2p}$ for $h\nu \geq 534.6$ eV [30]. At $h\nu \leq 530.1$ eV, E_{KLL} stays at constant E_B as indicated by a dotted vertical line in Fig. 4(b). The constant-initial-state (CIS) spectra of $E_B \leq 4.8$ eV are shown in Fig. 4(c). One can see that the CIS spectra of the IGSs ($E_B \leq 3.2$ eV) showed Fano profiles [34]: a local maximum was reached at $h\nu \sim 533.1$ eV with a preceding dip at $h\nu \sim 531.6$ eV [see also the intensity modulation at $E_B < 3$ eV in Fig. 4(b)]. On the other hand, the line shapes of the CIS spectra of the O $2p$ band region were similar to that of the absorption spectrum.

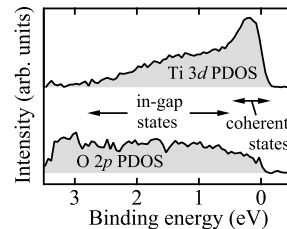


FIG. 5: Ti $3d$ and O $2p$ PDOSs of STO:Nb near E_F .

In Fig. 5, we show Ti $3d$ and O $2p$ PDOSs in the near- E_F regions derived from the resonant PES measurements. Here, the Ti $3d$ (O $2p$) PDOS is the difference between the spectra taken at $h\nu = 458.2$ eV (533.1 eV) and 450.4 eV (531.6 eV.) One can see that the IGSs consist of Ti $3d$ and O $2p$ states, whereas the coherent states mainly consist of Ti $3d$ states. The presence of Ti $3d$ character in the IGS shows that this structure cannot solely be attributed to Nb $4d$ donor levels.

If the IGSs of STO:Nb were formed by a spectral-weight transfer from the coherent states as schematically shown in Fig. 1(b), one would expect similar line shapes for the Ti $3d$ and O $2p$ PDOSs, which is apparently not the case as seen in Fig. 5. Therefore, one needs to explicitly consider the O $2p$ states as well as the Ti $3d$ states in explaining the coherent states and the IGSs. To this end, we adopt a local description of the electronic structure: the coherent states and IGSs originate from Ti sites initially having nominally- d^1 configuration (the same initial state to that of the Ti^{3+} peak in the Ti $2p_{3/2}$ spectrum). This interpretation is supported by the observation [8, 14] that the spectral weight of the region including the coherent states and the IGSs scales with x , which is similar to the Ti^{3+} -component weight in the Ti $2p_{3/2}$ spectra scaling with x [15]. Then, the mixed character of p and d in the IGSs can be explained as the final state composed of $d^1 \underline{L}$ (\underline{L} denotes a hole in the O $2p$ ligand orbital) and d^0 , since the former has p character while the latter has d character. The mixing of $d^1 \underline{L}$ into d^0 , which is a consequence of d - p hybridization, can alternatively be described that the Ti $3d$ -electron-emitted final state is partly screened by the electrons in the local ligand (O $2p$) orbitals. In fact, there is a recent trend to

understand the valence-band spectra in terms of screening orbitals [35, 36, 37], a concept originally developed to understand the core-level spectra [38]. The coherent state, on the other hand, is understood as a final state which is non-locally screened by a coherent band having mainly- d character [37, 39]. These assignments are similar to those adopted for LaTiO_3 [36] and $(\text{Ca,Sr})\text{VO}_3$ [37], although STO:Nb is a non-integer filling system.

Our assignment of the IGS to locally-screened incoherent state implies that there exists another incoherent state at higher E_B having poorly-screened character [Fig. 1(c).] Thus, the spectral weight of the coherent state of doped STO is transferred with increasing correlation ($x \rightarrow 1$) to the poorly-screened incoherent state as well as to the locally-screened state [see the electronic-structure evolution with x illustrated in Fig. 1(c).] This picture smoothly connects to the theoretical prediction [35] that the charge gap of the d^1 end member such as LaTiO_3 has intermediate character between Mott-Hubbard and charge-transfer-type due to strong d - p hybridization (see also [30, 37].)

It is well known that locally-screened final states, split off from the itinerant O $2p$ band, are similar to multiple charge states of transition-metal impurities in

semiconductors as proposed by Haldane and Anderson [19, 40, 41]. The present IGSs having locally-screened character are thus considered qualitatively equivalent to the multiple charge states. Here, the “impurity” site is the Ti site having a nominally- d^1 configuration embedded in the host STO. With increasing the hybridization between the impurity and the host, multiple charge states of the impurity accumulate in the middle of the band gap since the energy separation of different charge states becomes small due to increased screening, and also since the states are more strongly repelled from the valence band and the conduction band [19]. Hence, the IGS of electron-doped STO appearing in the middle of the band gap is understood as a result of strong d - p hybridization. We expect that a similar mechanism could be applicable to explain e.g. the in-gap states of electron-doped TiO_2 and the incoherent states positioned ~ 1 eV below E_F of the moderately correlated vanadates [37, 42, 43, 44, 45]. Direct investigation of O $2p$ states as demonstrated here or the search for poorly-screened final states will be the keys to prove this scenario.

We thank M. Takizawa, A. Fujimori, T. Yoshida and D.-Y. Cho for useful information and discussion.

-
- [1] M. Cardona, Phys. Rev. **140**, A651 (1965).
 [2] A. Ohtomo and H. Y. Hwang, Nature **427**, 423 (2004).
 [3] A. Brinkman, M. Huijben, M. van Zalk, U. Zeitler, J. C. Maan, W. G. van der Wiel, G. Rijnders, D. H. A. Blank, and H. Hilgenkamp, Nat. Mater. **6**, 493 (2007).
 [4] H. Ohta, S. Kim, Y. Mune, T. Mizoguchi, K. Nomura, S. Ohta, T. Nomura, Y. Nakanishi, Y. Ikuhara, M. Hirano, H. Hosono, and K. Koumoto, Nat. Mater. **6**, 129 (2007).
 [5] H. Nakamura, H. Takagi, I. H. Inoue, Y. Takahashi, T. Hasegawa, and Y. Tokura, Appl. Phys. Lett. **89**, 133504 (2006).
 [6] Y. Tokura, Y. Taguchi, Y. Okada, Y. Fujishima, T. Arima, K. Kumagai, and Y. Iye, Phys. Rev. Lett. **70**, 2126 (1993).
 [7] A. Fujimori, I. Hase, M. Nakamura, H. Namatame, Y. Fujishima, Y. Tokura, M. Abbate, F. M. F. de Groot, M. T. Czyzyk, J. C. Fuggle, O. Strebel, F. Lopez, M. Domke, and G. Kaindl, Phys. Rev. B **46**, 9841 (1992).
 [8] T. Yoshida, A. Ino, T. Mizokawa, A. Fujimori, Y. Taguchi, T. Katsufuji, and Y. Tokura, EuroPhys. Lett. **59**, 258 (2002).
 [9] T. Higuchi, T. Tsukamoto, K. Kobayashi, Y. Ishiwata, M. Fujisawa, T. Yokoya, S. Yamaguchi, and S. Shin, Phys. Rev. B **61**, 12860 (2000).
 [10] Y. Aiura, I. Hase, H. Bando, T. Yasue, T. Saitoh, and D. S. Dessau, Surf. Sci. **515**, 61 (2002).
 [11] D. D. Sarma, S. R. Barman, H. Kajueter, and G. Kotliar, EuroPhys. Lett. **36**, 307 (1996).
 [12] J. Zaanen, G. A. Sawatzky, and J. W. Allen, Phys. Rev. Lett. **55**, 418 (1985).
 [13] A. Fujimori, I. Hase, H. Namatame, Y. Fujishima, Y. Tokura, H. Eisaki, S. Uchida, K. Takegahara, and F. M. F. de Groot, Phys. Rev. Lett. **69**, 1796 (1992).
 [14] S. W. Robey, V. E. Henrich, C. Eylem, and B. W. Eichhorn, Phys. Rev. B **52**, 2395 (1995).
 [15] K. Morikawa, T. Mizokawa, A. Fujimori, Y. Taguchi, and Y. Tokura, Phys. Rev. B **54**, 8446 (1996).
 [16] A. Fujimori, A. E. Bocquet, K. Morikawa, K. Kobayashi, T. Saitoh, Y. Tokura, I. Hase, and M. Onoda, J. Phys. Chem. Solids **57**, 1379 (1996).
 [17] M. Imada, A. Fujimori, and Y. Tokura, Rev. Mod. Phys. **70**, 1039 (1998).
 [18] L. C. Davis, J. Appl. Phys. **59**, R25 (1986).
 [19] F. D. M. Haldane and P. W. Anderson, Phys. Rev. B **13**, 2553 (1976).
 [20] S. Ohta, T. Nomura, H. Ohta, M. Hirano, H. Hosono, and K. Koumoto, Appl. Phys. Lett. **87**, 092108 (2005).
 [21] H. Ohashi *et al.*, AIP Conf. Proc. **879**, 523 (2007).
 [22] M. Abbate, F. M. F. de Groot, J. C. Fuggle, A. Fujimori, Y. Tokura, Y. Fujishima, O. Strebel, M. Domke, G. Kaindl, J. van Elp, B. T. Thole, G. A. Sawatzky, M. Sacchi, and N. Tsuda, Phys. Rev. B **44**, 5419 (1991).
 [23] J. F. Herbst and J. W. Wilkins, Phys. Rev. Lett. **43**, 1760 (1979).
 [24] T. Higuchi, T. Tsukamoto, N. Sata, M. Ishigame, Y. Tezuka, and S. Shin, Phys. Rev. B **57**, 6978 (1998).
 [25] L. F. Mattheiss, Phys. Rev. B **6**, 4718 (1972).
 [26] G. Toussaint, M. O. Selme, and P. Pecheur, Phys. Rev. B **36**, 6135 (1987).
 [27] B. Reihl, J. G. Bednorz, K. A. Müller, Y. Jugnet, G. Landgren, and J. F. Morar, Phys. Rev. B **30**, 803 (1984).
 [28] F. M. F. de Groot, J. Faber, J. J. M. Michiels, M. T. Czyzyk, M. Abbate, and J. C. Fuggle, Phys. Rev. B **48**, 2074 (1993).
 [29] L. H. Tjeng, C. T. Chen, and S.-W. Cheong, Phys. Rev. B **45**, 8205 (1992).

- [30] J.-H. Park, PhD Thesis, Univ. of Michigan (1994).
- [31] O. Tjernberg, S. Söderholm, U. O. Karlsson, G. Chiaia, M. Qvarford, H. Nylén, and I. Lindau, *Phys. Rev. B* **53**, 10372 (1996).
- [32] Y. Tezuka, S. Shin, T. Uozumi, and A. Kotani, *J. Phys. Soc. Jpn.* **66**, 3153 (1997).
- [33] R. Ruus, A. Saar, J. Aarik, A. Aidla, T. Uustare, and A. Kikas, *J. Electron Spectrosc. Relat. Phenom.* **93**, 193 (1998).
- [34] U. Fano, *Phys. Rev.* **124**, 1866 (1961).
- [35] T. Uozumi, K. Okada, and A. Kotani, *J. Phys. Soc. Jpn.* **62**, 2595 (1993).
- [36] K. Okada, T. Uozumi, and A. Kotani, *J. Phys. Soc. Jpn.* **63**, 3176 (1994).
- [37] R. J. O. Mossaneck, M. Abbate, and A. Fujimori, *Phys. Rev. B* **74**, 155127 (2006).
- [38] J. C. Fuggle, M. Campagna, Z. Zolnierak, R. Lasser, and A. Platau, *Phys. Rev. Lett.* **45**, 1597 (1980).
- [39] M. Taguchi, A. Chainani, N. Kamakura, K. Horiba, Y. Takata, M. Yabashi, K. Tamasaku, Y. Nishino, D. Miwa, T. Ishikawa, S. Shin, E. Ikenaga, T. Yokoya, K. Kobayashi, T. Mochiku, K. Hirata, and K. Motoya, *Phys. Rev. B* **71**, 155102 (2005).
- [40] T. Mizokawa, A. Fujimori, H. Namatame, K. Akeyama, and N. Kosugi, *Phys. Rev. B* **49**, 7193 (1994).
- [41] M. A. van Veenendaal and G. A. Sawatzky, *Phys. Rev. Lett.* **70**, 2459 (1993).
- [42] I. H. Inoue, I. Hase, Y. Aiura, A. Fujimori, Y. Haruyama, T. Maruyama, and Y. Nishihara, *Phys. Rev. Lett.* **74**, 2539 (1995).
- [43] A. Sekiyama, H. Fujiwara, S. Imada, S. Suga, H. Eisaki, S. I. Uchida, K. Takegahara, H. Harima, Y. Saitoh, I. A. Nekrasov, G. Keller, D. E. Kondakov, A. V. Kozhevnikov, T. Pruschke, K. Held, D. Vollhardt, and V. I. Anisimov, *Phys. Rev. Lett.* **93**, 156402 (2004).
- [44] K. Maiti, D. D. Sarma, M. J. Rozenberg, I. H. Inoue, H. Makino, O. Goto, M. Pedio, and R. Cimino, *EuroPhys. Lett.* **55**, 246 (2001).
- [45] R. Eguchi, T. Kiss, S. Tsuda, T. Shimojima, T. Mizokami, T. Yokoya, A. Chainani, S. Shin, I. H. Inoue, T. Togashi, S. Watanabe, C. Q. Zhang, C. T. Chen, M. Arita, K. Shimada, H. Namatame, and M. Taniguchi, *Phys. Rev. Lett.* **96**, 076402 (2006).